JOURNAL OF OPTOELECTRONICS AND ADVANCED MATERIALS Vol. 9, No. 6, June 2007, p. 1653 - 1659

Effect of Ti, Ni and Bi addition to the corrosion resistance of Zn hot-dip galvanized coatings

N. PISTOFIDIS, G. VOURLIAS*, E. PAVLIDOU, G. STERGIOUDIS
Physics Department, Aristotle University of Thessaloniki, Thessaloniki, 54124 Greece

An usual phenomenon during zinc hot-dip galvanizing is the formation of coatings with extreme thickness and brittleness (Sandelin effect). This phenomenon is highly undesirable and for its inhibition titanium, nickel or nickel and bismuth are added in the zinc melt. The effect of these elements on the corrosion resistance of the zinc coatings is not yet investigated. In the present work the behavior of galvanized coatings containing 1%Ti, 1%Ni and 1%Ni-1%Bi was examined. The as-cast coatings were exposed in a Salt Spray Chamber, along with coatings deposited from a pure zinc bath for comparison purposes. The as-corroded coupons were characterized with Optical Microscopy, Scanning Electron Microscopy and X-Ray Diffraction. From this investigation it turned out that in every case the main corrosion products are hydrated zinc oxides and chlorides. Iron compounds were detected only at the final stage after 14 days of exposure. Pitting corrosion was also locally observed, but the predominant mechanism is uniform degradation. By contrast, the pure zinc coatings mainly suffer from pitting corrosion along with intergranular corrosion. In any case the corrosion performance after the addition of the alloying elements is enhanced.

(Received November 14, 2006; accepted April 26, 2007)

Keywords: Galvanizing, Coating, Zinc, Alloying elements, Corrosion, SEM, XRD

1. Introduction

Zinc hot-dip galvanizing is one of the most effective methods to protect steels against aqueous corrosion [1-7]. In this technique the ferrous substrate after the necessary surface treatment is immersed in a bath of molten zinc and as a result it is covered by a zinc coating with an average thickness of a few tens of μm [3-7]. When ferrous substrates are galvanized in a pure zinc bath at about 450 ^{o}C, the deposited coating consists of a succession of four layers referring to Γ, δ, ζ and η phase of the Fe-Zn phase diagram [3-7]. However, as the industrial steels differ from pure iron (α-Fe, ferrite), often different coating structure and morphology is observed, although the temperature and composition of the Zn melt is the typical. A well-studied phenomenon that has a significant effect on galvanized coatings is the Sandelin effect [8]. In this case, the high Si content of the ferrous substrate (>0.21%) along with the high P content could trigger the growth of thick layers with poor adhesion to the substrate. For the inhibition of this phenomenon the addition of different metallic elements in the Zn bath is examined [9-22]. Among them Ti seems to be very beneficial, because, apart from the fact that it reduces steel reactivity [9, 10, 12, 13, 15, 18], it is also more anodic than Zn (E^{o} (25^{o}C)=-0.762 V for Zn^{2+}/Zn, E^{o} (25^{o}C)=-1.630 V for Ti^{2+}/Ti [19]). Ni and Bi are also very effective for similar applications [14, 16, 17, 20-22]. The galvanized coatings formed when dipping steels in Ti added Zn baths have the typical structure [9, 10, 12, 13, 15]. However, at the ζ-η interface polyhedral dross particles are trapped which contain 4.5 wt.% Ti, 7.5 wt.% Fe and 88 wt.% Fe. Furthermore dross barriers (almost continuous lines of dross polyhedra) are present far from the ζ-η interface due to periodical precipitations occurring from successive Ti enrichments and impoverishments. However the addition of Ni and Bi alters significantly the coating morphology [16, 17, 22]. The coating produced from a zinc melt containing 1%Ni and 1% Bi is composed by three layers which, starting from the ferrous substrate, correspond to the δ phase of the Fe-Zn system, the T-phase of the Fe-Zn-Ni system and the η-phase of the Fe-Zn system. At the upper part of the coating large polyhedral inclusions of the T-phase are trapped, while Bi was detected only in the form of inclusions between the grains of the T-phase.

Nevertheless, although the above mentioned works are very detailed and accurate, they do not examine the corrosion performance of the Zn-Ti, Zn-Ni and Zn-Ni-Bi hot-dip coatings. Consequently the aim of the present research is the assessment of the corrosion resistance of these coatings, while an attempt is made for its correlation with the coating structure. As a result a brief overview of the coating structure is also presented, which refers to dipping time similar to that used in industrial scale facilities (a few minutes [7]).

2. Experimental procedure

Hot-rolled 3 mm thick sheets of steel containing 0.11% C, 0.55% Mn, 0.012% Si, 0.016% P have been galvanized in a laboratory electric furnace (Thermolyne 1400) inside a graphite crucible. The dipping time was set at 3 min. The coupons, 60 mm long and 7 mm wide, were degreased in a solution of a non-ionic tenside containing H_3PO_4, pickled (deoxidized) in an aqueous solution containing 16% HCl and fluxed in an aqueous solution containing 50% $ZnCl_2{\cdot}2NH_4Cl$, before their dipping in the galvanizing bath at a temperature of 450±2^{o}C. The

composition of the galvanizing baths is summarized in Table I. In the case of Ti the presented composition was selected because this is the maximal Ti solubility according to the Ti-Zn phase diagram [23]. A pure Zn bath at the same temperature was used as a reference for the reproduction of the typical morphology of galvanized coatings. All metals and materials used (apart from the steel coupons) were of laboratory grade.

Table 1. Composition of the galvanizing baths.

Bath No	Bath composition
1	Zn-0.5wt.% Ti
2	Zn-1.0 wt.% Ni
3	Zn-1.0 wt.% Ni-1.0 wt.% Bi
Ref.	Zn

For the study of the corrosion performance the as-cast specimens were hanged vertically with nylon fibers at about the center of the working volume of a Salt Spray Chamber (SSC) SC-450 Umwelttechnik GmbH. The corrosive medium was a 5 wt. % solution of NaCl in de-ionized water. The temperature of the chamber was 40^{o}C while the relative humidity remained stable at 100%.

Specimens were retrieved from the chamber after 48, 144, 240 and 336 hrs (2, 6, 10 and 14 days respectively). For the examination of the morphology of the specimens prior and after corrosion, cross sections have been cut from the galvanized coupons, mounted in bakelite, polished down to 5 μm alumina emulsion, etched in a 2% Nital solution (2% HNO_3 in CH_3CH_2OH) and observed with an Olympus BX60 light microscope connected with a digital camera CCD JVC TK-C1381. The nature of the phases formed was determined with X-ray diffraction (XRD) and scanning electron microscopy (SEM) associated with an EDS analyser. For the XRD experiments a 2-cycles SEIFERT 3003 TT diffractometer (CuKα radiation) with Bragg-Brentano geometry was used, while the SEM study was accomplished with a 20kVolt JEOL 840A SEM equipped with an OXFORD ISIS 300 EDS analyzer and the necessary software for point microanalysis, linear microanalysis and chemical mapping of the surface under examination. For the examination of the corrosion progress the weight of the coatings was measured prior and after the exposure in the SSC, while the corroded samples were examined with a Karl Zeiss M8 stereoscope equipped with a CCD camera for image capture. Furthermore the weight of the coated specimens was measured prior and after the exposure in the SSC and the percentage of the weight change was calculated following the equation:

%Weight Change = 100 * (Initial Weight - Final Weight) / Initial Weight

3. Results

Characteristic SEM micrographs of the cross-section of the above-mentioned coatings are presented in Fig. 1. The observed morphology is more or less in accordance with the litterature data [9-22]. In every case three layers could be distinguished based on their relief. In contact with the ferrous substrate, a thin zone is observed which is expanded along the steel surface. In this phase cracks are present which are perpendicular to the substrate surface. EDS analysis implies that it refers to the δ-phase of the Fe-Zn phase diagram. A thicker layer follows, which, in the case of the Zn-Ti coating, probably corresponds to the ζ-phase of the same phase diagram, while in the coatings containing Ni corresponds to the T-phase of the Fe-Zn-Ni phase diagram. On top of it, every coating is sealed by the η-phase of the Fe-Zn system. Ti and Ni were detected in the η-phase with a relatively uniform distribution, while Bi was present only in the form of small inclusions. Furthermore in every case polyhedral dross inclusions were observed scattered in the eta phase. From the above examination it seems that the coating structure is more or less similar, especially as far as it concerns the outer part which is initially exposed to the corrosive environment. Consequently similar corrosion performance is expected. In any case, for the corrosion study the coated coupons were exposed in SSC. This experiment resulted in every case to the formation of voluminous corrosion products on the galvanized surface, as the stereographic photographs of Fig. 2 show about the coatings formed in a Zn-Ti bath. This observation was also quantitatively verified as the diagrams of Fig. 3 show, since in every case a slight increase of the weight of the coated samples is recorded. Nevertheless, the weight change during corrosion, even in simulated and well controlled environments, depends on several factors such as the specimen geomentry, its exact position in the SSC, the speed of the NaCl-solution jet etc [24] and as a result this conclusion could not be generalized. In any case, from the macroscopic examination of all samples after their retrieval from the SSC it could be concluded that their degradation began even from the beginning of exposure. The EDS analysis of the lateral surface of the samples retrieved after 48 hrs showed that zinc (Zn), oxygen (O) and chlorine (Cl) at different concentrations composed the corrosion products. Consequently, zinc oxides and chlorides had been already formed from the second day of exposure, as it was also verified with XRD. However, red rust (iron oxides) appeared on the surface of the samples galvanized in baths with alloying elements, only after of 14 days of exposure and their quantity was very low. By contrast, on the samples galvanized in a pure Zn bath, a large volume of iron oxides was formed after the same period of time (Fig. 2e). The formation of these oxides is either due to the iron content of the coating which ranges from 0.03% up to 27% with regard to the distance from the Fe/Zn interface [3], either due to the exposure of the ferrous substrate because of coating failure. However in this case, the quantity of the oxide formed is so high that the exposure of the substrate is a necessary fact for its explanation. Nevertheless, since corrosion is a localized phenomenon, the observed failure is also localized at the points where the coating was characterized by defects. In any case, the fact that red rust was not observed on the Ti-galvanized coatings implies that the corrosion resistance of these coatings is superior to that of the coatings galvanized in pure Zn.

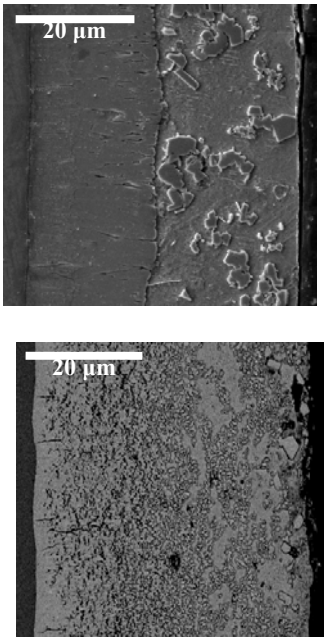

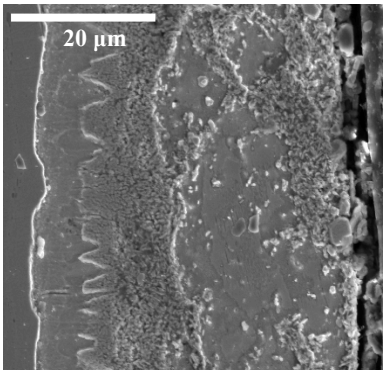

Fig. 1. *SEM micrographs of the cross-section of the coating formed from a Zn-0.5wt.% Ti bath (a), Zn-1.0wt. % Ni-1.wt.% Bi bath (b) and Zn-1.0wt.% Ni bath (c).*

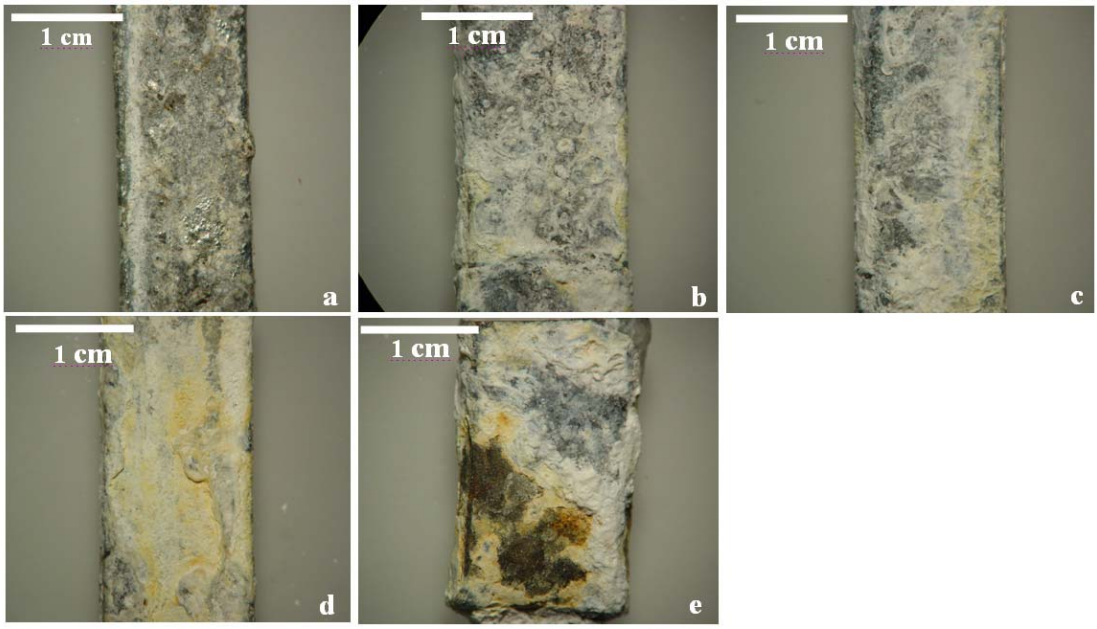

Fig. 2. Stereographic photo-graphs of the corroded specimens galvanized in a Zn-1.0wt.% Ti bath after 2 (a), 6 (b), 10 (c) and 14 (d) days of exposure and stereographic photograph (e) of a sample galvanized in pure Zn after 14 days of exposure.

This observation was also verified with the examination of the cross-section of the specimens with optical microscopy (Fig. 4-7).

The corrosion of the coatings galvanized in Zn alloys is much lighter and thus their resistance is superior. Pitting corrosion occurs along with uniform corrosion [24], but the substrate is not exposed. Pitting corrosion is very usual when SSC is used, because this corrosion form is highly affected by the oxygen content of the electrolyte (water).

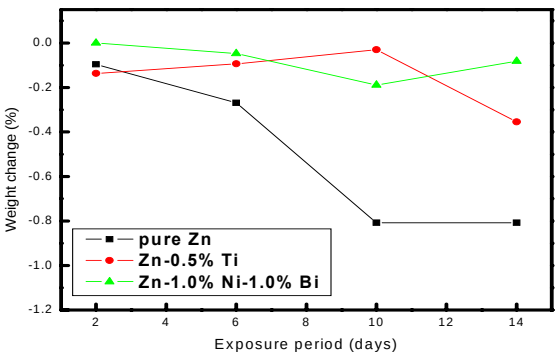

Fig. 3. Weight change of the corroded samples after the exposure in the SSC.

The water used in SSC, because of the constant spraying at which it is submitted, is obviously saturated in oxygen when it comes in contact with the examined coupons. This phenomenon enhances pitting procedure. The presence of high concentration of Cl^- ions is also another factor that facilitates pitting. Cl^- can cause breakdown of the passive film which covers galvanized coatings when exposed in the open air [24]. By contrast the corrosion of the samples galvanized in pure Zn, although it seems to progress with the same mechanism, is severe. After 14 days the coating is decomposed, while its thickness is strongly decreased. However in this case a mechanism of intergranular corrosion is also likely to be present as Fig. 7b and 7c show. In this case the Cl^- ions diffuse preferentially through the grain boundaries of the coating and react with zinc forming different water-soluble zinc compounds leading to the detachment of grains. Furthermore under these circumstances diffusion of the corroded species through the inherent crack network of the delta phase is possible [25-26]. As a result the degradation of the zinc coating is accelerated.

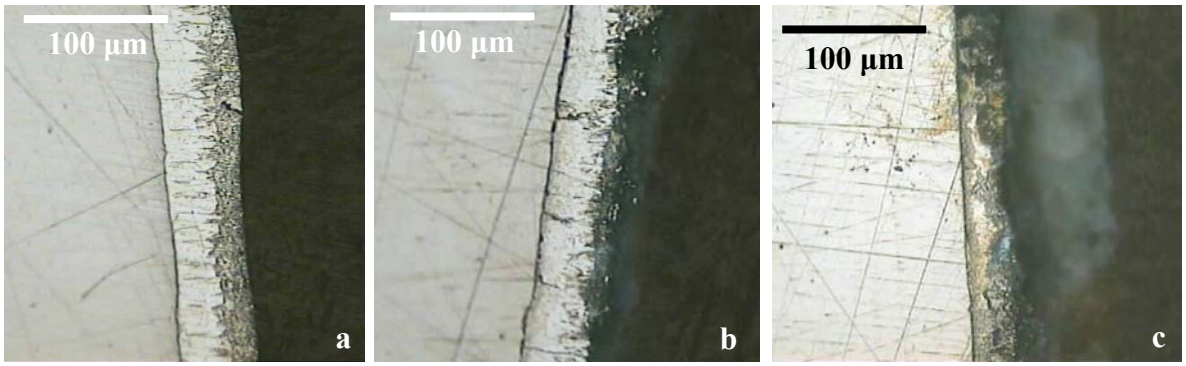

Fig. 4. Optical micrographs of the corroded samples formed with 1.0 wt.% Ti after 2 (a), 10 (b) and 14 (c) days of exposure in the SSC.

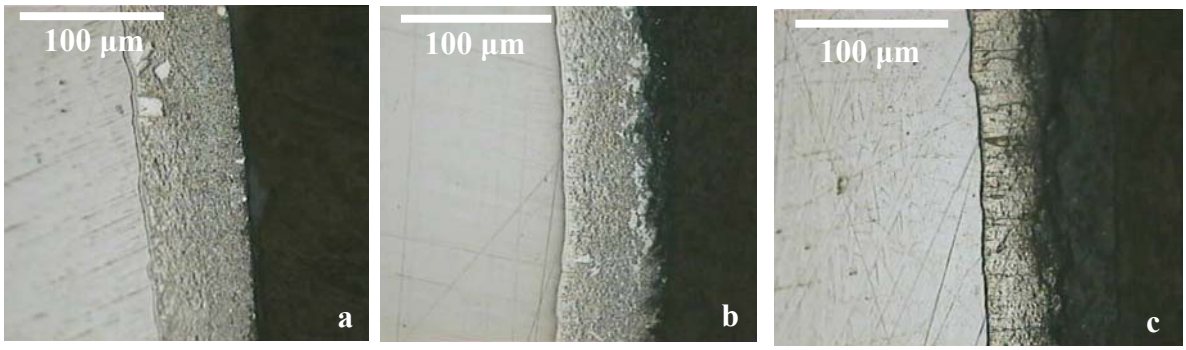

Fig. 5. Optical micrographs of the corroded samples formed with 1.0 wt.% Ni and 1.0wt.% Bi after 2 (a), 10 (b) and 14 (c) days of exposure in the SSC.

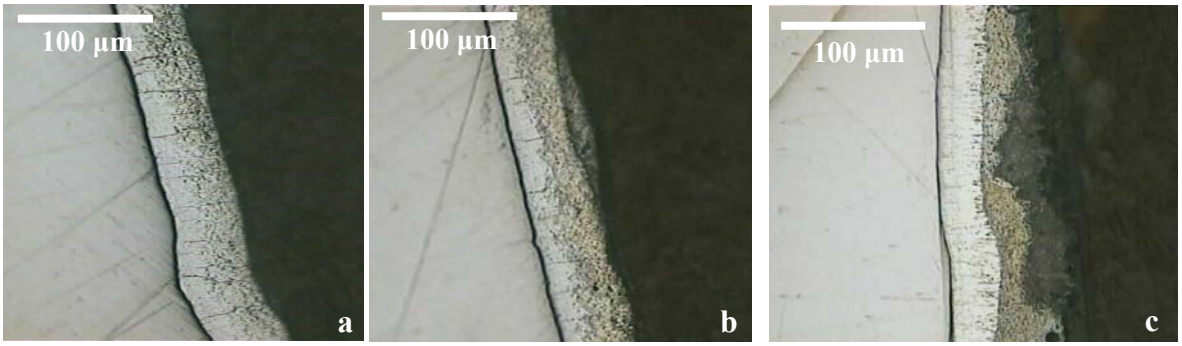

Fig. 6. Optical micrographs of the corroded samples formed with 1.0 wt.% Ni after 2 (a), 10 (b) and 14 (c) days of exposure in the SSC.

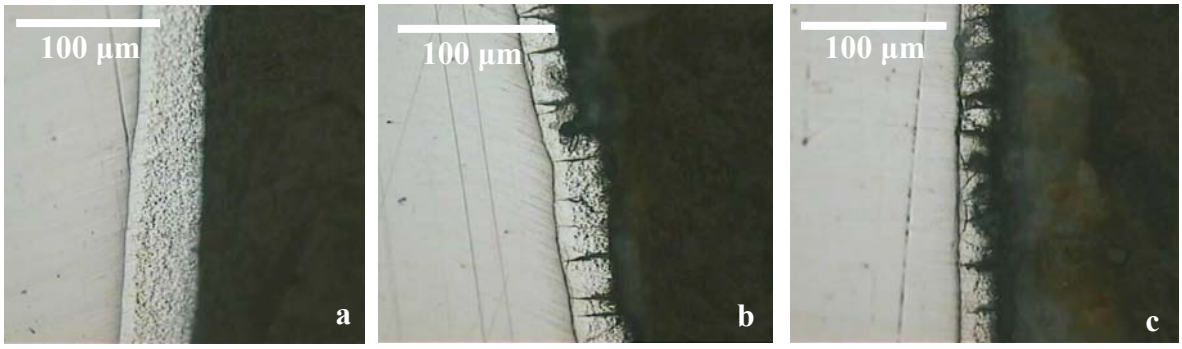

Fig. 7. Optical micrographs of the corroded samples formed in a pure Zn bath after 2 (a), 10 (b) and 14 (c) days of exposure in the SSC.

For a better understanding of the corrosion progress the cross-section of the samples was examined with SE microscopy. A representative SEM micrograph of the coating formed from a Zn-Ti bath after 14 days of exposure is presented in Fig. 8 along with the EDS analysis of the area under examination. As the optical micrographs have already shown, mostly the upper part of the coating is attacked. A large volume of corrosion products is gathered on top of it with almost the same thickness with the substrate. The underlying part is also affected and large pits are formed with high concentration of oxygen and chlorine ions. However the lower part of the coating is not attacked. It still looks compact and adherent to the ferrous substrate, while, as the chemical mapping of the same figure shows, the aggressive ions (oxygen and chlorine) are not diffused in it. As a result the substrate is still protected. Similar conclusions could be drawn for the coatings formed from Zn melts containing Ni and Ni-Bi (Fig. 9-10). Pitting and uniform corrosion is observed also in this case, while a thick layer of corrosion products is present with chemical composition similar to the one earlier reported. Although the coating is heavily affected, the substrate is still protected. By contrast the attack of the coatings galvanized in pure Zn after the same exposure period is much more severe. The coating thickness is very low, while oxygen and chlorine are diffused up to iron.

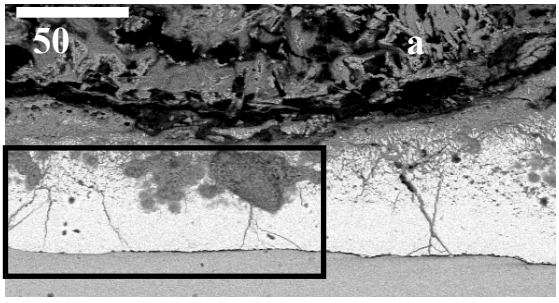

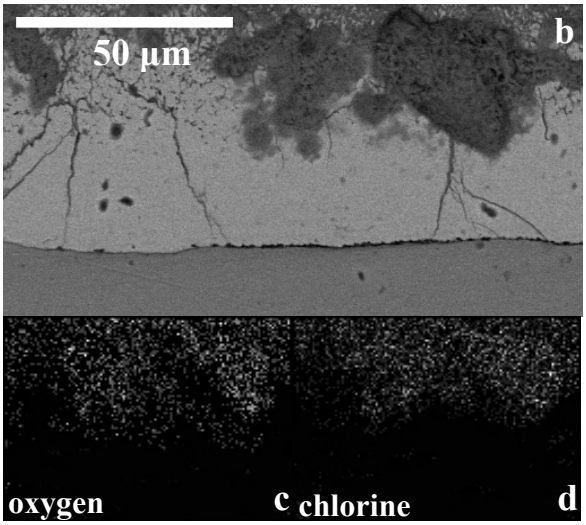

Fig. 8. SEM micrographs (at low (a) and higher (b) magnification) of the cross-section of the corroded coating formed from a Zn bath with 1.0 wt.% Ti after 14 days of exposure in the SSC and elemental mapping of the same area. The brighter areas correspond to higher concentration of oxygen (c) and chlorine (d).

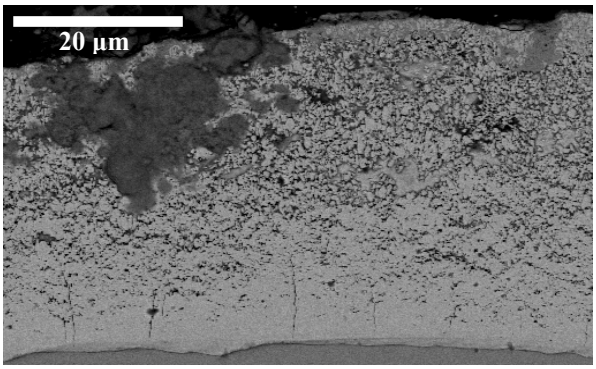

Fig. 9. SEM micrograph of the cross-section of the corroded coating formed from a Zn bath with 1.0 wt.% Ni and 1.0 wt.% Bi after 14 days of exposure in the SSC.

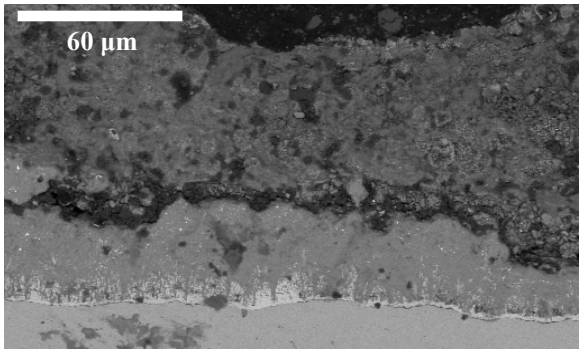

Fig. 10. SEM micrograph of the cross-section of the corroded coating formed from a Zn bath with 1.0 wt.% Ni after 14 days of exposure in the SSC.

The data of the EDS analysis could also offer useful information about the aggressiveness of the Cl^- ions with regard to the exposure time. The analysis is oriented to that ionic specie because it is the most aggressive, since its compounds are highly soluble in water and as a result they facilitate corrosion. On the other hand oxygen compounds are water insoluble and thus they do not promote the coating degradation. Hence the presence of Cl^- is detrimental for the coating performance and therefore their penetration is very critical. To calculate this value their compositional profile was measured after 14 days of exposure with EDS for every sample as Fig. 11 shows. From this plot it is obvious that Cl^- ions are spread up to the Fe/Zn interface in the case of pure Zn coatings, although for the other coatings the penetration depth is much lower. The pure Zn coating curve is interrupted at about 40 μm from the Fe/Zn interface because the thickness of this coating is lower with regard to the others due to the faster decomposition. The penetration depth is different for every alloyed coating but in every case is of the same order of magnitude. Similar analysis for lower exposure time shows that Cl^- concentration in the coatings increases constantly as a function of the time of exposure. The relation however, between the different curves, remains almost constant. Hence the addition of the alloying elements seems to enhance the performance of the coatings.

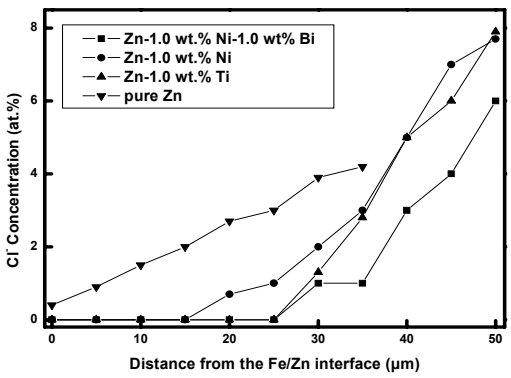

Fig. 11. Distribution of the Cl^- ions at the cross-section of the different coatings after 14 days of exposure in the SSC.

The improved corrosion performance of the Ti-alloyed zinc coatings with regard to pure Zn could be assigned to the fact that Ti is anodic to zinc [19]. Consequently corrosion is delayed since Ti acts synergistically with zinc, which behaves as a cathode and thus protected. Bi, on the other hand, is more cathodic than zinc [19]. However Bi unlikely Ni and Ti is not dispersed in the coating, but it is observed only in the form of inclusions. As a result it does not affect corrosion unless one of these inclusions is exposed. The effect of Ni is more complicated. Although Ni is less reactive than zinc [19] and consequently it was supposed to accelerate zinc corrosion, it seems to have a protective role. This phenomenon could be attributed to the formation of a superficial oxide layer that isolates the coating acting as a barrier between the coating and the aggressive environment.

4. Conclusions

From the above investigation it was concluded that:

1. The addition of Ti, Ni or Ni-Bi in the zinc melt improves the corrosion performance of the hot-dip galvanized coatings. Pitting and uniform corrosion are the predominant corrosion mechanisms.
2. Pure Zn coatings are much more susceptible. In this case, apart from pitting and uniform corrosion, possibly intergranular corrosion also takes place.
3. In every case the corrosion products consist of Zn and Fe oxides and chlorides.

References

[1] E. Mattson, Basic Corrosion Technology for Scientists and Engineers, 2d Edition, IOM Communications, London (1996).
[2] M.G. Fontana, Corrosion Engineering, 3d Edition, McGraw-Hill, New York (1986).
[3] A.R. Marder, Prog. in Mat. Sci. **45**, 191(2000).
[4] ASM Handbook, Hot Dip Coatings, Vol. 13-Corrosion, New York (1999).
[5] Galvanizers Association, The engineers and architects' guide to hot dip galvanizing, Sutton Coldfield, Great Britain (2000).
[6] American Galvanizers Association, Galvanizing for Corrosion Protection-A Specifier's Guide, Colorado (2000).
[7] P. Maass, P. Peissker, Handbuch Feuerverzinken, Wiley-VCH (1993).
[8] ILZRA, Galvanizing Reactive Steels-A guide for Galvanizers and Specifiers, N. Carolina (1996).
[9] G. Reumont, T. Gloriant, P. Perrot, J. Mat. Sci. Lett. **14**, 752(1995).
[10] G. Reumont, T. Gloriant, P. Perrot, J. Mat. Sci. Lett. **15,** 445(1996).
[11] G. P. Lewis, J. Pedersen, Proc. 3rd Asian Pacific Galvanizing Conf., Australia, Cominco Ltd, (1996), p. 1.

[12] G. Reumont, T. Gloriant, P. Perrot, J. Mat. Sci. Lett. **16,** 62(1997).
[13] T. Gloriant, G. Reumont, P. Perrot, Z. Metallkd. **88**, 539(1997).
[14] G. Reumont, P. Perrot, J. Foct, J. Mat. Sci. **33**, 4759(1998).
[15] J.D. Culcasi, P.R. Sere, C.I. Elsner, A.R. Di Sarli, Surf. Coat. Tech. **122**, 21(1999).
[16] N.Y. Tang, X. Su, J.M. Toguri, Calphad **25**, 267(2001).
[17] R. Fratesi, N. Ruffini, M. Malavolta, T. Bellezze, Surf. Coat. Tech. **157**, 34(2002).
[18] G.P. Vassiliev, X. J. Liu, K. Ishida, J. All. Comp. **375**, 162 (2004).
[19] CRC Handbook of Chemistry and Physics, Ed. D.R. Lide, 80th Ed., CRC Press, London (1999-2000).
[20] M. Gagne, Bull. Bis. Inst. **72**, 1(1998).
[21] S. M. A. Shibli, R. Manu, Surf. Coat. Tech. **197**, 103(2005).
[22] N. Pistofidis, G. Vourlias, S. Konidaris, El. Pavlidou, G. Stergioudis, Mat. Lett., submitted for publication (2006).
[23] J. L. Murray, Bull. Alloy Phase Diag. **5,** 21(1984).
[24] X. G. Zhang, Corrosion and Electrochemistry of Zinc, Plenum Press, NewYork (1996).
[25] G. Vourlias, N. Pistofidis, G. Stergioudis, E. Pavlidou, D. Tsipas, Phys. Stat. Sol. A, **201**, 1518(2004).
[26] G. Reumont, J. B. Vogt, A. Iost, J. Foct, Surf. Coat. Tech. **139**, 265(2001).

*Corresponding author: gvourlia@auth.gr